Bicycle Wheel System Identification and Optimal Truing Control for Mechatronic Systems

Aaron Hunter

***Abstract*—This paper describes an *in-situ* empirical modeling technique of a conventional bicycle wheel that is employed to determine the optimal tension adjustments necessary to align the wheel in lateral and radial directions while maintaining uniform tension of the spokes. The technique allows the mean tension of the spokes to be adjusted independently from variations around the mean. Additionally, a control algorithm is developed that uses lateral feedback and predicted intermediate wheel states to bring the wheel into alignment to any desired tension in a single iteration of adjustments of the tension of the spokes. Experimental validation of the algorithm is demonstrated on a poorly tensioned and misaligned wheel summarized here:**

Parameter	Inital ($\mu \pm \sigma$)	Final ($\mu \pm \sigma$)
Lateral [mm]	0.160 ± 0.736	-0.037 ± 0.107
Radial [mm]	0.050 ± 0.158	-0.046 ± 0.047
Tension [N]	556 ± 211	1009 ± 45

***Index Terms*—IEEE, IEEEtran, journal.**

I. Introduction

THE spoked bicycle wheel is one of the most ubiquitous tensioned structures in the world. While much has been written about modeling the structure itself (see [1] for a comprehensive literature review) very little has been published regarding the assembly and tuning of the structure itself. This work presents a framework for a rigorous approach to empirically modeling a bicycle wheel and provides for an optimal tensioning method for all wheels of the same type. This framework is intended for integration into a mechatronic wheel manufacturing apparatus although the results presented here were produced by hand, albeit with the assistance of measurement sensors and a computer.

The approach presented in this paper builds upon the one patented by Papadapolous [2] and alluded to in [3] for the wheel tensioning method. This approach is to determine the influence of a tension adjustment of each spoke on the lateral, radial and spoke tension parameters of a specific wheel. These influence functions are placed into a model in matrix form. This model is then employed to compute a weighted least squares estimation of the tension adjustments that minimize the wheel parameter variations for a given wheel under tensioning. Where this work improves upon previous approaches is to provide tension targeting and a method for feedback control during the tensioning process to minimize cumulative adjustment errors.

A. Hunter is a PhD student at the Department of Computer Science and Engineering, University of California, Santa Cruz, CA, 95060 USA e-mail: aamuhunt@ucsc.edu.

Manuscript received month day, year; revised month day, year.

II. Background

The bicycle wheel structure consists of a rim, spokes, spoke nipples, and a hub as shown in Fig(1). The hub anchors the spoke which is connected to the rim by a nipple threaded onto its end and seated in the rim. The wheel structure is placed under tension, which provides its stiffness and strength, by adjusting the nipples until the desired tension is achieved. Lateral stiffness of the wheel is provided by the lateral component of the spoke tension due to the spoke angles α_{nd} and α_d. Lateral stiffness prevents rim warping out of the wheel plane and allows for minimization of lateral variations. Radial stiffness and compensation is provided by the radial component of the spoke tension. The optimal tension of the wheel is a balance between the two, that is, high enough tension to support the anticipated load, but below the value that begins to induce rim warpage [1]. Note that there are two other degrees of freedom for rim displacements: tangential (rim compression along the circumference) and torsion around the rim shear center. The former acts to reduce the circumference of the rim, however, this effect is difficult to measure due to the very high stiffness of the rim in this direction. For purposes of this work we consider the rim incompressible in the tangential direction. The latter might be of concern for wheels containing spokes significantly offset from the rim center and thus generating a twisting moment. In this work, however, we assume that any torsion effect is minimized when the lateral and radial variations are minimized. In practice, these effects are primarily reduced through appropriate rim design.

Spoking patterns vary from purely radial to nearly tangential relative to the hub and determined by angle β. Tangential spoke patterns allow for torque transmission from the hub to the rim, which occurs through the drive train or from disc brakes. With the exception of front wheels for use with rim brakes most wheels are built with some amount of tangential spoking.

The process of adjusting the tension to minimize the lateral and radial variations of the wheel is called truing. The typical procedure for wheel truing by hand is a heuristic where first some average spoke tension is applied by tightening all the spoke nipples, then the lateral variations are iteratively reduced, and finally the radial variations are minimized. The wheel tension is then increased incrementally and the procedure is repeated until the wheel parameter specifications are met [4].

The wheel can be modeled as a system of springs operating in a linear regime [1]. Because of this linear property, the wheel parameter variations induced by the spokes can be de-

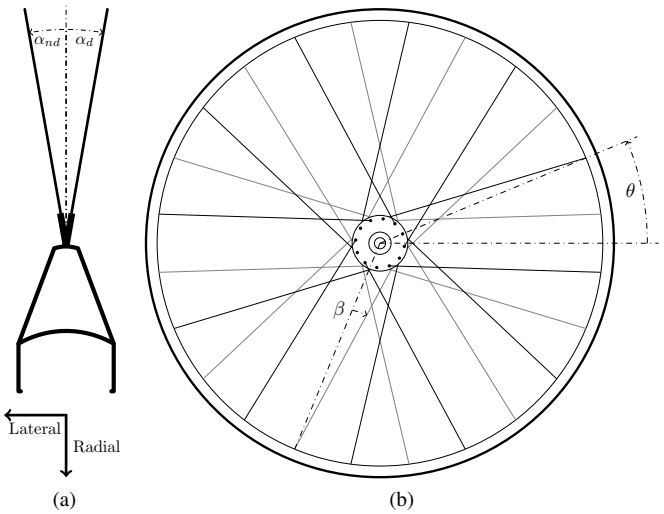

Fig. 1. Wheel geometry. (a) Rim cross section. The lateral direction is defined to point toward the non-drive side of the wheel. The radial direction points outwards from the hub. The spoke angles α_{nd} and α_d provide lateral stiffness to the wheel. (b) Side view of a wheel. The rim angle, θ, is referenced to the valve stem. The angle, β, results from the wheel spoke pattern, A purely radially spoked wheel has $\beta = 0$.

composed into superposed individual spoke tensions, lending itself to influence matrix approach developed later in this work.

III. Apparatus

To develop the model a symmetric (i.e., tensioned equally on both sides), front wheel was built by hand using a Stans ZTR Alpha rim, a White Industries MI5 hub, and 32 DT Swiss Competition spokes. A so-called 'three-cross' tangential spoke pattern was employed for the wheel geometry. All adjustments were performed on a Centrimaster Comfort wheel truing stand (Fig 2). This stand has radial and lateral mechanical dial gauges to measure the rim displacements with 0.1 mm gauge markings. To obtain optimal resolution and minimize data collection time, a Canon EOS M digital camera with a 22mm focal length lens was used to capture images from the dial gauges. A computer vision algorithm was used to analyze the images and calculate the displacements. The spoke tension measurements were taken with a WheelFanatyk digital tension gauge. This instrument measures the lateral displacement of a spoke by a known spring tension. This displacement is converted to a measured tension based on a lookup table provided by the manufacturer. It has a claimed accuracy of 10% and the measurements are discretized to 0.01 mm.

IV. Method

A. Wheel Model

The approach taken here is to determine the effect of a constant change in spoke tension on the lateral, radial and tension parameters of a wheel as a function of rim angle. The resulting curves are referred to as the influence functions of the spoke. To find these influence functions a series of experiments are performed on a subset of the spokes in a given wheel. For each experiment a spoke is loosened by one complete rotation

Fig. 2. Apparatus used to measure lateral and radial displacements.

and measurements are taken at equal increments along the rim, for the radial and lateral displacements, and the tension of every spoke is measured. The data are used to develop the influence functions, The influence functions for each spoke are then placed into matrix forms such that each column represents the influence of a given spoke and each row represents a discrete rim angle. In other words, if $u_s(\theta), v_s(\theta),$ and $t_s(\theta)$ are the lateral and radial influence functions for spoke $s \in [1, 2, \cdots, n_s]$, then the influence matrices Φ_u, Φ_v and Φ_t for the lateral, radial and tension parameters respectively, at the discrete rim angles $\theta \in [\theta_1, \theta_2, \cdots, \theta_n]$ are given by:

$$\mathbf{u_s} = \begin{bmatrix} u_s(\theta_1) \\ u_s(\theta_2) \\ \vdots \\ u_s(\theta_n) \end{bmatrix} \mathbf{v_s} = \begin{bmatrix} v_s(\theta_1) \\ v_s(\theta_2) \\ \vdots \\ v_s(\theta_n) \end{bmatrix} \mathbf{t_s} = \begin{bmatrix} t_s(\theta_1) \\ t_s(\theta_2) \\ \vdots \\ t_s(\theta_n) \end{bmatrix}$$

$$\begin{aligned} \Phi_u &= \begin{bmatrix} \mathbf{u_1} & \mathbf{u_2} & \dots & \mathbf{u_{n_s}} \end{bmatrix} \\ \Phi_v &= \begin{bmatrix} \mathbf{v_1} & \mathbf{v_2} & \dots & \mathbf{v_{n_s}} \end{bmatrix} \\ \Phi_t &= \begin{bmatrix} \mathbf{t_1} & \mathbf{t_2} & \dots & \mathbf{t_{n_s}} \end{bmatrix} \end{aligned}$$

The influence matrices are the models of the wheel for each parameter. We combine these matrices into a single matrix Φ:

$$\Phi = \begin{bmatrix} \Phi_u \\ \Phi_v \\ \Phi_t \end{bmatrix} \tag{1}$$

Given a vector of tension adjustments (i.e., rotations of the spoke nipples), $\mathbf{d}$, the prediction of the wheel state after applying the adjustments is given by:

$$\hat{\mathbf{Y}} = \mathbf{Y_b} + \Phi\mathbf{d} \tag{2}$$

where $\hat{\mathbf{Y}}$ is the predicted state of the wheel after tensioning and $\mathbf{Y_b}$ is the state of the wheel prior to tensioning.

To find the optimal vector of spoke tension adjustments, $\mathbf{d}_{ls}$, that result in a measured state relative to a perfect wheel at average tention $\bar{T}$ we solve the weighted least squares

approximation using a set of measurements $[\mathbf{u}, \mathbf{v}, \mathbf{T} - \bar{T}]$, and the weights μ_v and μ_t:

$$\tilde{\Phi} = \begin{bmatrix} \Phi_u \\ \Phi_v\sqrt{\mu_v} \\ \Phi_t\sqrt{\mu_t} \end{bmatrix} \quad \tilde{\mathbf{Y}} = \begin{bmatrix} \mathbf{u} - u_0 \\ (\mathbf{v} - v_0)\sqrt{\mu_v} \\ (\mathbf{T} - \bar{T})\sqrt{\mu_t} \end{bmatrix} \tag{3}$$

$$\mathbf{d}_{ls} = \tilde{\Phi}^{\dagger}\tilde{\mathbf{Y}} \tag{4}$$

Where $\tilde{\Phi}^{\dagger}$ is the pseudo-inverse of $\tilde{\Phi}$. Typically u_0 and v_0 are zero reflecting the fact that the gauge has been set to zero at the desired lateral and radial locations during setup. The weighting factors represent the tradeoff between the lateral, radial, and tension variables and account for the difference in units, the quality of measurements (magnitude and relative noise contribution), as well as the specification for each parameter. The weighting factors are determined through simulation and validated experimentally. Once $\mathbf{d}_{ls}$ is found the wheel is trued to its optimal state, $\hat{\mathbf{Y}}_{ls}$ by applying $\mathbf{d}_{adj} = -\mathbf{d}_{ls}$ to the wheel:

$$\hat{\mathbf{Y}}_{ls} = \mathbf{Y}_{\mathbf{b}} + \Phi\mathbf{d}_{adj} \tag{5}$$

B. Tension Targeting

In theory adjusting a wheel to an arbitrary average tension can be accomplished by setting $\bar{T} = T_d$ in (3), where T_d is the desired tension. As will be demonstrated later, however, the tension influence functions are noisy and lack the necessary precision to target tension accurately. Therefore a better method is needed to simultaneously true and tension a wheel to T_d. For this method we exploit the wheel symmetry and make the following observation. If every spoke of a symmetric wheel is tightened by the same amount then the radial and lateral displacements are unaffected and only the mean tension is changed. It is possible therefore to decouple the average tension change from spoke tension non-uniformity. It should be apparent that this is possible for asymmetric wheels as well, such as a drive wheel or wheel with a disc brake, by compensating for the different spoke angles.

The approach is as follows. First calculate $\mathbf{d}_{ls}$ as in (4) and subtract its mean value. This is the spoke adjustment vector which will cause a perfectly true wheel to result in the measured wheel state, but without incurring an average tension shift. As before, $\mathbf{d}$ is the vector that transforms the wheel to the trued state:

$$\mathbf{d} = -(\mathbf{d}_{ls} - \bar{d}_{ls})$$

If the adjustments, $\mathbf{d}$, are applied to the spokes, the lateral, radial and tension variations will be minimized as before, but without changing the average tension. To determine the necessary constant shift d_{cm} to bring the average tension to T_d we calculate the following :

$$d_{cm} = (T_d - \bar{T})/c$$

Where the proportionality constant, c, is determined experimentally as the change in tension of the wheel when all the spokes are rotated by one revolution and has units N/rev. The spoke vector that will optimally true the wheel is:

$$\mathbf{d}_{adj} = \mathbf{d} + d_{cm} \tag{6}$$

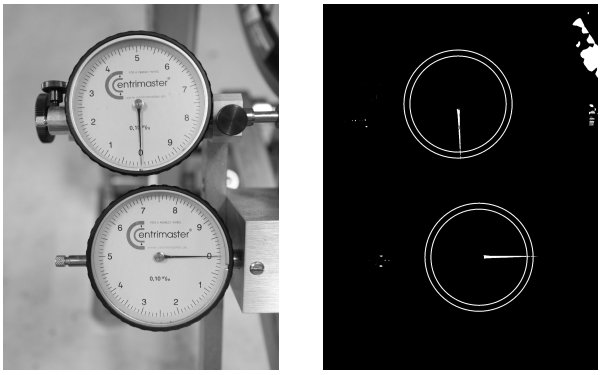

(a) (b)

Fig. 3. Images used to measure analog dial gauges with computer vision. Image (a) is the measurement image. Image (b) is generated by subtracting the measurement image from a reference image and applying binary threshold and masking operations (concentric circles). The angle of the needles is measured relative to the gauge center and the converted to a displacement measurement.

C. Optical Digitization

The method for converting the analog dial gauge readings into digital measurements merits some discussion. Although a mechatronic implementation of a wheel tensioning machine would likely use digital gauges, it is instructive to demonstrate the effectiveness of optical digitization. Prior to taking measurements two images are collected. The first is a reference image taken with the gauge needles outside the range of expected data range. The second image is taken with the needles set to zero. With these two images any subsequent image of a measurement is processed in the following manner. The measurement image is subtracted from the reference image after appropriate smoothing. If the images are taken under the same conditions, what remains after subtraction is a ghost image of the needles themselves. A binary threshold is applied to the subtracted image and masked. Finally, the centroid of the needle tip is determined and an angle from the gauge center to the tip is calculated and compared to the measurement at zero. The angle is then converted into displacement using the gauge resolution. This process is demonstrated in Fig(3).

D. Wheel Truing Algorithm

Having determined the optimal spoke adjustments, $\mathbf{d}_{adj}$, the remaining task is to apply them to the wheel. Although this sounds deceptively simple, there are some difficulties doing this accurately. The main one is a problem of spoke twist. Spokes are not torsionally stiff and will twist significantly during nipple rotation. Thus it is difficult to determine precisely how far the spoke nipple has been adjusted based entirely on the rotation angle of the spoke nipple. The servo accuracy or precision may also be inadequate, leading to the accumulation of errors over multiple spoke adjustments. This is particularly true at higher spoke tensions where the friction of the nipple-spoke interface can lead to discrete jumps in nipple rotation. Finally, even if the nipple has been adjusted properly but the spoke is twisted, over time it can un-twist which may result in tension loss of the spoke and cause the wheel to go out of true.

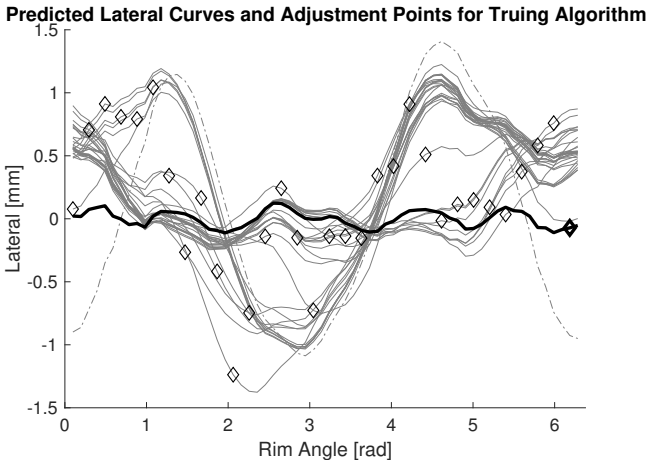

Fig. 4. Example of the truing algorithm. The dashed line is the baseline lateral state. The thin lines are the predicted states after each spoke adjustment. The spoke tension is adjusted until the lateral measurement equals the diamond target and proceeds from the first spoke (leftmost) to the last. The thick line is the predicted final state with its truing target.

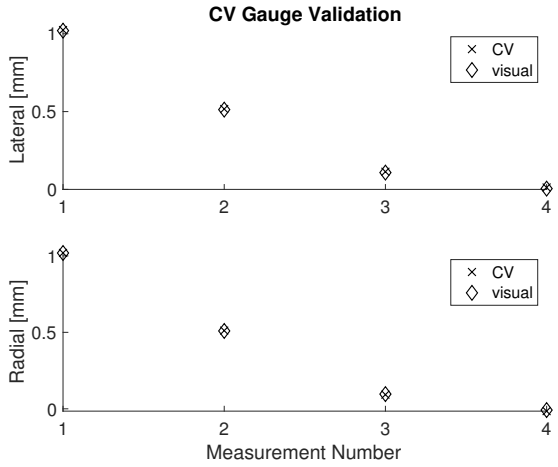

Fig. 5. Validation of the computer vision algorithm developed to interpret analog dial gauge measurements. Both the lateral and radial dials were set to approximately 1, 0.5, 0.25, and 0.0mm. The measurements were interpreted through visual estimation of the images as well as by the algorithm. The results agree to better than the estimate of the resolution of the manual technique.

Although the use of high precision servos and clamping the spoke during adjustment improve the wheel truing process, this paper demonstrates a method that minimizes these sources of variability using lateral feedback during each spoke adjustment. The method begins with the first element of $\mathbf{d}_{adj}$. Using (2) the post-adjustment lateral displacement at the rim angle of that spoke is predicted for the target displacement. The spoke tension is then adjusted until the lateral measurement equals the target displacement. Spoke twist is eliminated by measuring the spoke rotation hysteresis during adjustment and setting the spoke nipple angle midway in the hysteresis regime. Note that this lateral target displacement is not zero, but rather the intermediate state of the wheel after the adjustment of the first spoke. Then a prediction is made of the lateral state at the rim angle of the second spoke after the first *two* adjustments have been performed. The second spoke tension is adjusted until the target is reached in the same manner of the first. This process continues sequentially for every element in $\mathbf{d}_{adj}$. This method minimizes any accumulation of adjustment error while eliminating spoke twist. Fig(4) shows the predicted lateral states of a wheel after each spoke adjustment along with the lateral targets (diamond symbols). These targets were used to true the wheel for the experiment shown in Fig(15) in the next section. The dashed line represents the lateral state of the wheel prior to tuning, the thin lines show each intermediate state prediction, and the thick line is the prediction of the final state. The algorithm applies each adjustment from the spoke with the smallest angle proceeding sequentially to the spoke at the highest rim angle. In practice some adjustments will be too small to perform and can be safely ignored if the wheel state at that spoke already agrees with the target within an acceptable tolerance.

V. Results

A. Optical Digitization of Lateral and Radial Measurements

To provide for higher precision measurements and to automate analog to digital conversion of the analog dial gauge measurements a computer vision algorithm was employed. To validate the measurement reliability a series of four images were taken. They were first analyzed for their readings manually (through pixel level measurement of the angle of the needles) and then compared against the results returned by the algorithm. Both dial gauges were set to approximately the following settings: 1.0 mm, 0.5 mm, 0.25 mm, and 0.0 mm. Fig(5) shows the comparison between the two methods. The estimated effective displacement resolution of the manual measurement method is approximately 0.014 mm. The computer vision algorithm returned values within ± 0.007 mm of the manual measurements.

B. Influence Functions

Influence functions were measured for every spoke, 32 in total, where the spoke was loosened by one complete rotation of the spoke nipple. For each influence function the lateral and radial displacements were measured at 64 equally spaced locations on the rim–at and midway between each spoke location. To minimize spoke twist in the estimation of the rotation, the spokes and nipples were marked prior to the rotation. A full rotation of the nipple brought the marks back into alignment. These curves were averaged (after normalizing them to the same rim angle) and in the case of the radial displacement, the mean value subtracted. As stated earlier this is due to our assumption that the rim is incompressible in the tangential direction, thus a tension change does not change the average radius. The subsequent influence functions are shown in Fig(7). For each tension influence function the tension of every spoke was measured after one spoke was loosened by a full rotation, thus each tension influence function has 32 measurements. This particular spoking geometry results in four

distinct tension patterns, depending on whether the spoke is on the drive side of the wheel, or the non-drive side, and whether it is a 'leading' spoke or a 'trailing' spoke, that is whether its spoke angle, β, is positive or negative (see Fig(1). Because this is a symmetric wheel, however, the non-drive side leading spoke influence function is a mirror image of the drive side trailing one. Similarly, the non-drive side trailing spoke influence function is a mirror image of the drive side leading one. This symmetry was exploited to generate the four tension influence functions in Fig(8), such that each function represents the average of 16 measured curves and is mirrored when necessary.

The lateral and radial influence functions can be used directly and put into the influence matrices. Alternatively, they can be fit to the Fourier series which is an ideal modeling method for these functions due to their continuous nature and 2π periodicity. The Fourier series takes the form:

$$y(\theta) = a_0 + \sum_{n=1}^{N} a_n \cos(n\theta) + b_n \sin(n\theta)$$

where $n\theta$ is the spatial frequency of the mode of oscillation and $y(\theta)$ is the function to be fitted. To develop the model of these functions the set of measured influence functions were randomly divided into two sets, a modeling set and a testing set. The modeling set were fit to the Fourier series to find the coefficients a_n, b_n. The highest significant spatial frequency was determined by plotting the sum squared residual error between the modeling and testing sets against the number of fitting coefficients, and therefore spatial frequency. This is plotted in Fig(6). It is evident from this plot that the residual error for the lateral influence function is reduced in the testing data set up to a spatial frequency, $N_{lat} = 6$ (i.e., 13 fitting coefficients) and up to $N_{rad} = 13$ (27 fitting coefficients) for the radial influence function. Because the mean influence functions of Fig(7) exhibit little noise, they were used for the model in this work. If there were fewer measured functions, however, using the modeled approach would be more appropriate.

The tension measurements are inherently discrete so modeling them as a Fourier series, while feasible, has no meaning. There are analytical models available for them (see [5] for an open source example), however, they require extensive characterization of the rim that is not practical *in-situ*. Therefore, for this work only the smoothed data were used for the influence matrices.

Regardless of whether the model or the data are used in the influence functions, however, it should be clear that when constructing the influence matrices they will be less than full rank. This can be understood because the highest order spatial frequency that appears in the model is 13, corresponding to 27 basis vectors associated with the Fourier coefficients. This satisfies our intuitive understanding of the wheel structure particularly the fact that there are two degrees of freedom that are not taken into account in the wheel model, namely the tangential stiffness and the torsional stiffness of the rim, and that the mean tension of the wheel can be changed without affecting any of the displacement parameters. This

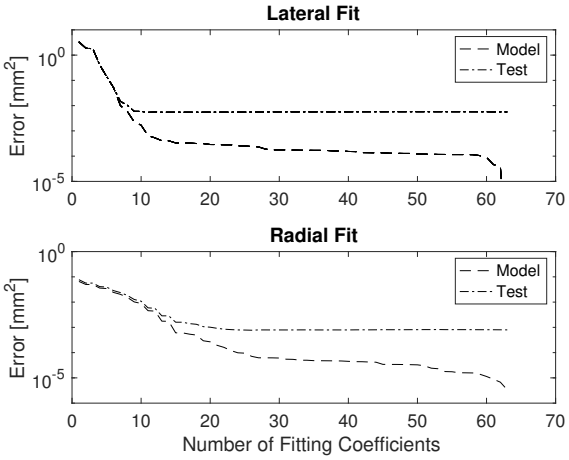

Fig. 6. Residual error vs fitting coefficient number for the lateral and radial influence functions when fit to a Fourier series. The residual of the testing set is used to determine the highest spatial frequency to be used for the model. Although difficult to discern due to the log scale, the residual error increases in the lateral testing set for fitting coefficients beyond 13, corresponding to $N_{lat} = 6$. Similarly the highest mode of oscillation for the radial influence function is determined to be $N_{rad} = 13$.

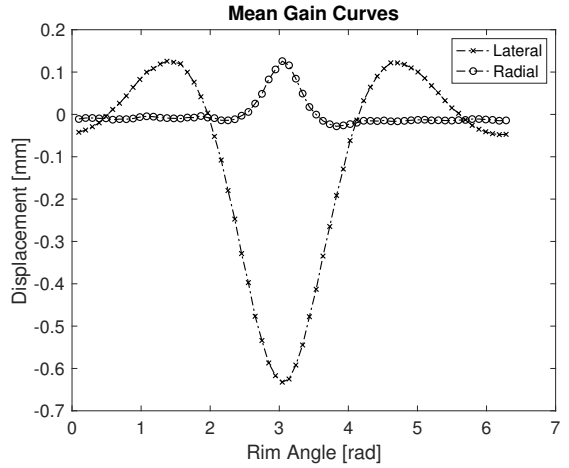

Fig. 7. The mean influence functions for the lateral and radial parameters. These functions are the average of 32 measured curves after normalizing them to the angle of the 16th spoke.

can be independently verified by performing a singular value decomposition of the influence matrices composed of solely averaged data for the influence functions, shown in Fig(9). It is evident that without the inclusion of the tension influence matrix the model of the wheel is underdetermined.

C. Simulation

With the influence matrices developed as in (1) the state of the wheel can be predicted for a given set of spoke tension adjustments. To find acceptable values for the weighting factors, μ_v, μ_t, a series of simulations were performed. For each simulation a random vector of spoke adjustments was generated and a wheel state prediction was calculated using (2). To this wheel state white noise was added to simulate the uncertainty of the measurement. The noise distributions were determined from the measured profiles generated during the

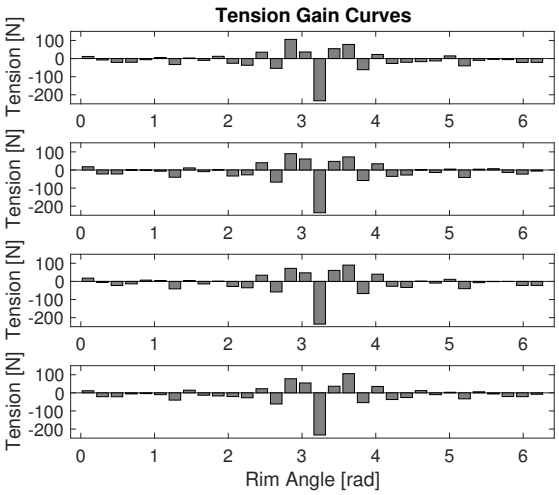

Fig. 8. The mean influence functions for spoke tension. From top to bottom: (a) Non-drive side leading. (b) Drive-side leading. (c) Non-drive side trailing. (d) Drive side trailing. Note that (a) and (d) are mirror images, as are (b) and (c).

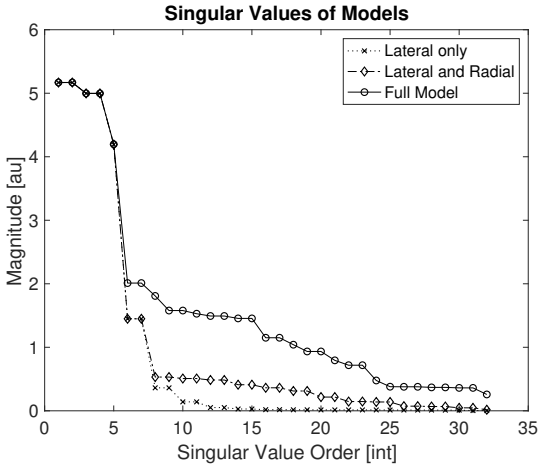

Fig. 9. The singular values associated with the singular value decomposition of the following influence matrices: lateral, the concatenation of the lateral and the radial, and the full model.

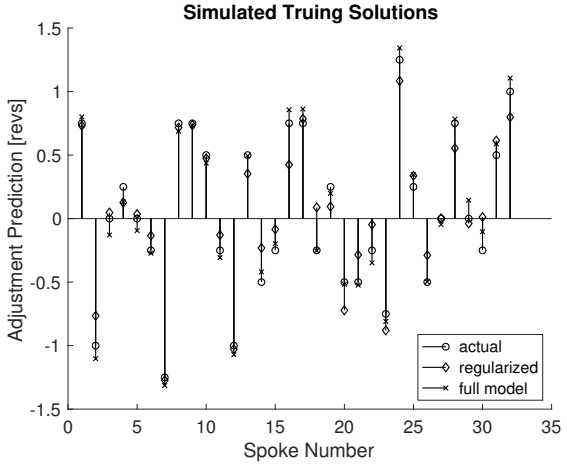

Fig. 10. Example of the simulation process used to determine the weighting factors for the multi-objective least squares approximation. The circles represent the actual spoke adjustments for a given simulation and the other symbols represent the approximations from two different approaches: a regularized model and the full model. On average, regularization resulted in estimation errors $2\times$ worse than when using the full model.

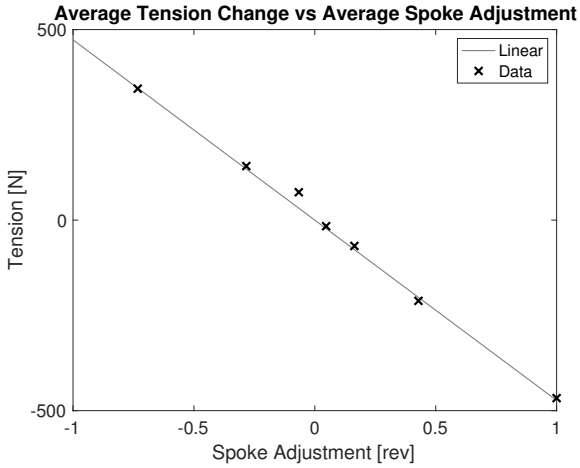

Fig. 11. The average tension change of a wheel due to the average spoke adjustment. A linear fit to the data finds $c = -473N/rev$.

influence function development. The initial weighting factors were developed based on a comparison of the magnitude of the changes induced by a unit disturbance of the three parameters, normalized to the maximum lateral displacement. The weighted least squares estimation of the random spoke vector was then computed using these weighting factors and (4). and the predicted final state of the wheel is calculated using (5). The weighting factors were then modified until both the predicted performance of the algorithm met a specification of $\pm$ 0.1mm in lateral and radial error and $\pm$50 N in tension error relative to a perfectly true wheel. The predicted spoke vector is generally found to agree to an rms of $\leq$ 0.1 revolutions. Fig(10) shows the result of one such simulation. After extensive simulation acceptable weighting factors were found to be: $\mu_v = 0.5$, $\mu_t = 10^{-5}$.

D. Model Validation

The model is separated into two parts, spoke adjustments which affect the variations in the wheel parameters while preserving the mean tension, and adjustments which affect the mean tension of the wheel but do not affect parameter uniformity. The latter part of the model is found by determining the coefficient, c, between the average of the spoke adjustment vector and the average tension change of the wheel. Fig(11) demonstrates the results of seven experiments. A linear fit to these data finds $c = -473$ N/rev. In practice, this constant could be derived from a single experiment where every spoke is adjusted by one revolution.

To validate the model performance for spoke adjustment vectors that affect the variations in the wheel parameters while preserving the mean tension, a different experiment was performed. In this case a random spoke adjustments vector was applied to the (manually trued) test wheel and the

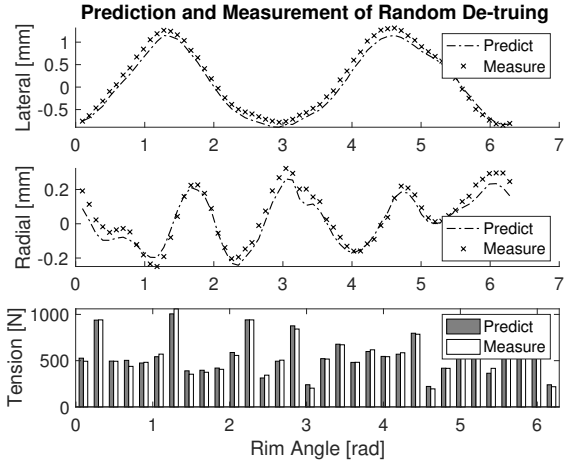

Fig. 12. The actual and predicted lateral, radial, and tension values for the random de-truing experiment.

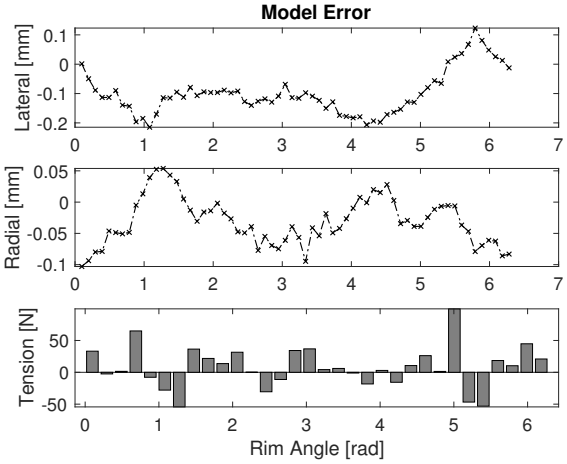

Fig. 13. The model error relative to the measurements for the random de-truing experiment. The rms errors are found to be 0.123 mm (lateral), 0.049 mm (radial), and 33 N (tension).

TABLE I
RESULTS OF CHANGING TENSION

Parameter	Inital ($\mu \pm \sigma$)	Final ($\mu \pm \sigma$)
Lateral [mm]	-0.029 ± 0.083	0.045 ± 0.063
Radial [mm]	-0.052 ± 0.032	-0.056 ± 0.039
Tension [N]	781 ± 33	1126 ± 76

resulting measured wheel parameters were compared to the model predictions. The truing algorithm was used to accurately make the spoke adjustments. Fig(12) shows the result of this experiment and Fig(13) shows the residual error of model after the adjustment. The rms model error of the lateral, radial and tension parameters are found to be 0.123mm, 0.049mm, and 33N, respectively. The model fits the data well considering the tolerance of the lateral adjustment which is estimated to be approximately 0.1mm.

Finally, to demonstrate the need for separating the model into two parts is demonstrated in Fig(14). For this experiment, a well-trued wheel tensioned to an average of 780N was given a new tension target of 1000N using (3). The subsequent spoke adjustment vector was applied to the wheel. The results of this experiment are summarized in Table(I). Although the wheel is still true the tension target has been exceeded by 126N and the tension non-uniformity is $1.5\times$ worse than the initial state in percentage terms (4.2% vs 6.8%). The reason for the failure of the model in this regime appears to be related to the tension influence functions themselves and is likely due to the relative large discretization errors of the tension measurement (nearly 4% at 1000N). Without finer resolution these discretization errors accumulate when a constant value is added to the spoke adjustment solution. Although better instrumentation and rigorous analysis of the influence functions would likely improve the results, separating the average tension change from the model works well, particularly as the average tension change is easily characterized as shown already.

E. Wheel Truing Validation

To validate the complete model and truing algorithm the de-trued wheel from the first experiment was trued to a target

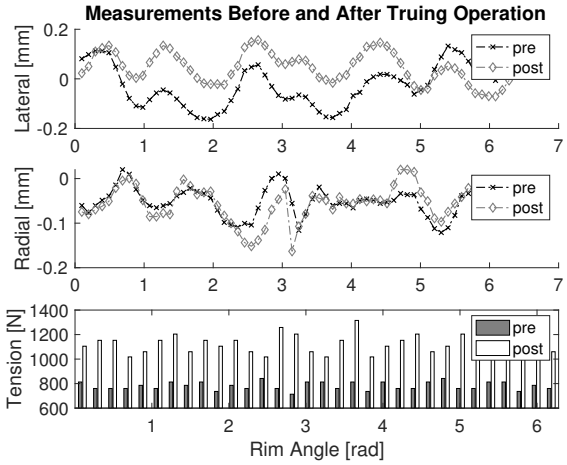

Fig. 14. Changing the tension of true wheel using the model described in (3). Although the wheel remains true the tension target of 1000N is significantly exceeded and has more variability.

TABLE II
TRUING ALGORITHM RESULTS

Parameter	Inital ($\mu \pm \sigma$)	Final ($\mu \pm \sigma$)
Lateral [mm]	0.160 ± 0.736	-0.037 ± 0.107
Radial [mm]	0.050 ± 0.158	-0.046 ± 0.047
Tension [N]	556 ± 211	1009 ± 45

tension of 1000 N. Fig(15) shows the wheel state before and after the truing operation and Table(II) summarizes the measurements. The maximum variations are 0.17 mm above the mean (lateral), 0.07 mm above the mean (radial), and 104 N below the mean (tension).

Finally, to see whether the performance of the truing algorithm could improve the wheel from the truing experiment was trued again. The results are shown in Table(III). The performance is modestly improved for every parameter.

VI. CONCLUSION

These results successfully demonstrate that a linear wheel model can be developed empirically using standard system

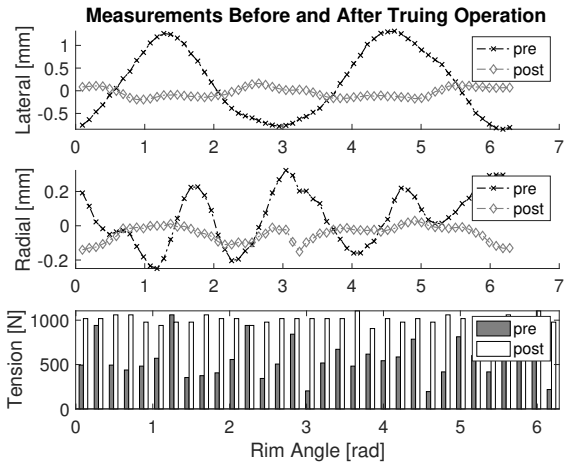

Fig. 15. The state of the wheel is shown before and after the truing operation. The results are summarized in Table(II).

TABLE III
SECOND ITERATION OF TRUING

Parameter	Inital ($\mu \pm \sigma$)	Final ($\mu \pm \sigma$)
Lateral [mm]	-0.037 ± 0.107	0.028 ± 0.073
Radial [mm]	-0.046 ± 0.047	-0.031 ± 0.034
Tension [N]	1009 ± 45	989 ± 39

identification methodology. This methodology consists of perturbing the wheel with known tension changes and measuring the resulting wheel state. An optimal spoke tension adjustment vector can be found using weighted linear least squares analysis of the wheel errors. This vector represents the best estimate for the adjustments necessary to true the wheel. The weighting factors are determined by an analysis of their relative magnitudes as well as to meet a desired specification. In addition, the mean spoke tension can be separated from the spoke variation around the mean. This allows accurate tension targeting even with relatively large errors in the tension influence matrix.

A truing algorithm that minimizes adjustment errors using a prediction of intermediate wheel states after adjustment of each spoke and lateral measurement feedback was demonstrated. This algorithm trues a wheel in a single iteration even to a significantly different tension. A second iteration of the truing algorithm can bring a small but significant improvement. The truing algorithm is also effective at minimizing spoke twist by detecting the hysteresis in the spoke nipple rotation and adjusting the nipple to the approximate midpoint of the hysteresis region once the lateral target is reached.

The main limitation to the model is the inaccuracy and perhaps more importantly the coarse discretization of the tension measurements. Because of this, the tension parameter is weighted relatively less than the radial and lateral parameters. The resulting wheel states after a truing operation reflect this weighting and the tension errors away from the target tension approach 10% in the worst case. The main limitation to the truing algorithm is the precision of the spoke tension adjustment. Some spoke nipples didn't rotate smoothly on the test wheel, particularly at high tension. Rather the nipple rotated in small discrete jumps as torque was applied. Thus the error in the lateral target adjustment approached 0.1mm. Using new components and appropriate lubrication would improve the precision of the adjustment and likely result in better performance. Even despite these limitations, the test wheel was trued to tight specifications.

To improve upon the tension performance a higher resolution and more repeatable tension measurement is desired. One approach that has been suggested (ref Papadopoulos) is to estimate the frequency the first vibrational mode of the spoke after plucking the spoke as one would a guitar string. The frequency is proportional to the square root of the tension thus the tension can be measured acoustically. Another alternative is to measure the torque required to adjust the spoke. The tension can be determined from the torque. However, this approach is sensitive to lubrication as well as mechanical imperfections of the components and may not be as reliable. An alternative to measuring the spoke tension is to use a regularization technique instead of a full influence matrix. Regularization places a cost on the amount of tension adjustment which is minimized along with the lateral and radial errors. This was approach was tested in simulation and found to have higher error than using the tension influence matrix.

As an aside, In this work an optical digitization of analog dial gauges was demonstrated to provide high precision measurements, at least as good as a pixel-level evaluation of images of the dial gauges. This technique provides an effective alternative to digital gauges.

ACKNOWLEDGMENT

The authors would like to thank Matthew Ford for modeling discussions and Stuart Davis of Santa Cruz Bicycles for providing the initial inspiration for the study.

REFERENCES

[1] M. Ford, "Reinventing the wheel: Stress analysis, stability, and optimization of the bicycle wheel," Ph.D. dissertation, Northwestern University, 2018.
[2] J. J. M. Papadopoulos, "Method for trueing spoked wheels," U.S. Patent 5 103 414A, Apr. 07, 1992.
[3] R. P. BegheynEef and P. F. Vermeulen, "Method and apparatus for aligning a wheel." Netherlands Patent 1 016 171C2, Mar. 15, 2002.
[4] J. Brandt, *The Bicycle Wheel*. Avocet, 1993.
[5] M. Ford. bike-wheel-calc. [Online]. Available: https://github.com/dashdotrobot/bike-wheel-calc

PLACE PHOTO HERE

Aaron Hunter Biography text here.

John Doe Biography text here.

Jane Doe Biography text here.